

Lattice QCD Calculations of Transverse-Momentum-Dependent Soft Function through Large-Momentum Effective Theory

Qi-An Zhang,¹ Jun Hua,² Yikai Huo,^{2,3} Xiangdong Ji,^{1,4} Yizhuang Liu,¹ Yu-Sheng Liu,¹ Maximilian Schlemmer,⁵ Andreas Schäfer,⁵ Peng Sun,⁶ Wei Wang,^{2,*} and Yi-Bo Yang^{7,8,9,†}

(Lattice Parton Collaboration)

¹Shanghai Key Laboratory for Particle Physics and Cosmology, MOE Key Laboratory for Particle Astrophysics and Cosmology, Tsung-Dao Lee Institute, Shanghai Jiao Tong University, Shanghai 200240, China

²INPAC, Shanghai Key Laboratory for Particle Physics and Cosmology, MOE Key Laboratory for Particle Astrophysics and Cosmology, School of Physics and Astronomy, Shanghai Jiao Tong University, Shanghai 200240, China

³Zhiyuan College, Shanghai Jiao Tong University, Shanghai 200240, China

⁴Department of Physics, University of Maryland, College Park, Maryland 20742, USA


⁵Institut für Theoretische Physik, Universität Regensburg, D-93040 Regensburg, Germany

⁶Nanjing Normal University, Nanjing, Jiangsu, 210023, China

⁷CAS Key Laboratory of Theoretical Physics, Institute of Theoretical Physics, Chinese Academy of Sciences, Beijing 100190, China

⁸School of Fundamental Physics and Mathematical Sciences, Hangzhou Institute for Advanced Study, UCAS, Hangzhou 310024, China

⁹International Centre for Theoretical Physics Asia-Pacific, Beijing/Hangzhou, China

 (Received 3 June 2020; revised 25 August 2020; accepted 7 October 2020; published 3 November 2020)

The transverse-momentum-dependent (TMD) soft function is a key ingredient in QCD factorization of Drell-Yan and other processes with relatively small transverse momentum. We present a lattice QCD study of this function at moderately large rapidity on a $2 + 1$ flavor CLS dynamic ensemble with $a = 0.098$ fm. We extract the rapidity-independent (or intrinsic) part of the soft function through a large-momentum-transfer pseudoscalar meson form factor and its quasi-TMD wave function using leading-order factorization in large-momentum effective theory. We also investigate the rapidity-dependent part of the soft function—the Collins-Soper evolution kernel—based on the large-momentum evolution of the quasi-TMD wave function.

DOI: [10.1103/PhysRevLett.125.192001](https://doi.org/10.1103/PhysRevLett.125.192001)

Introduction.—For high-energy processes such as Higgs production at the Large-Hadron Collider, quantum chromodynamics (QCD) factorization and parton distribution functions (PDFs) have been essential for making theoretical predictions [1,2]. But for processes involving observation of a relatively small transverse momentum Q_\perp , such as in Drell-Yan (DY) production and semi-inclusive deep inelastic scattering, a new nonperturbative quantity called “soft function” is required to capture the physics of non-canceling soft gluon radiation at fixed Q_\perp [3–6]. Physically, the soft function in DY production is a cross section for a pair of a high-energy quark and antiquark (or gluon) traveling in the opposite light-cone directions to

radiate soft gluons of total transverse momentum Q_\perp before they annihilate. Although much progress has been made in calculating the soft function in perturbation theory at $Q_\perp \gg \Lambda_{\text{QCD}}$ [7,8], it is intrinsically nonperturbative when Q_\perp is $\mathcal{O}(\Lambda_{\text{QCD}})$. Calculating the nonperturbative transverse-momentum-dependent (TMD) soft function from first principles became feasible only recently [9].

The main difference in such a calculation in lattice QCD is that it involves two lightlike Wilson lines along directions $n^\pm = (1/\sqrt{2})(1, \vec{0}_\perp, \pm 1)$ in (t, \perp, z) coordinates, making direct simulations in Euclidean space impractical. However, much progress has been made in recent years in calculating physical quantities, such as light-cone PDFs using the framework of large-momentum effective theory (LMET) [10,11]. The key observation of LMET is that the collinear quark and gluon modes, usually represented by lightlike field correlators [12–15], can be accessed for large-momentum hadron states. A detailed review of LMET and its applications to collinear PDFs and other light-cone distributions can be found in Refs. [16,17]. More

Published by the American Physical Society under the terms of the [Creative Commons Attribution 4.0 International license](https://creativecommons.org/licenses/by/4.0/). Further distribution of this work must maintain attribution to the author(s) and the published article's title, journal citation, and DOI. Funded by SCOAP³.

recently, some of the present authors have proposed that the TMD soft function can be extracted from a special large-momentum-transfer form factor of either a light meson or a pair of quark-antiquark color sources [9]. Once calculated, the TMD factorization of the Drell-Yan and similar processes can be made with entirely lattice QCD computable nonperturbative quantities [18–23].

The TMD soft function is often defined and applied not in momentum space but in transverse coordinate space in terms of the Fourier transformation variable b_\perp . In addition, it also depends on the ultraviolet (UV) renormalization scale μ (often defined in dimensional regularization and minimal subtraction or $\overline{\text{MS}}$) and rapidity regulators $Y + Y'$ [9,12],

$$S(b_\perp, \mu, Y + Y') = e^{(Y+Y')K(b_\perp, \mu)} S_I^{-1}(b_\perp, \mu), \quad (1)$$

where the first factor is related to rapidity evolution [described by the Collin-Soper (CS) kernel K], and the second factor S_I is the intrinsic rapidity-independent part of the soft contribution. The rapidity-regulator-independent CS kernel K is found calculable by taking the ratio of the quasi-transverse-momentum-dependent parton distribution function (TMDPDF) at two different momenta [20–25]. On the other hand, calculating the intrinsic soft function on the lattice has never been attempted before.

In this Letter, we present the first lattice QCD calculation of the intrinsic soft function S_I with several momenta on a $2 + 1$ flavor CLS ensemble with $a = 0.098$ fm [26], see Table I. In particular we perform simulations of the large-momentum light-meson form factor and quasi-TMD wave functions (TMDWFs), whose ratio gives the intrinsic soft function [9]. The Wilson loop matrix element will be used to remove the linear divergence in the quasi-TMD wave function. The CS kernel K can also be calculated from the external momentum dependence of the quasi-TMD wave function [16], and we will calculate it as a by-product. Our result is consistent with that of quenched lattice calculations of TMDPDFs [25].

Theoretical framework.—The intrinsic soft function (S_I) can be obtained from the QCD factorization of a large-momentum form factor of a nonsinglet light pseudoscalar meson with constituents $\pi = \bar{q}_2 \gamma_5 q_1$, with the transition

TABLE I. Parameters used in the numerical simulation. The first row shows the parameters of the $2 + 1$ flavor clover fermion CLS ensemble (named A654) and the second one shows the number of the A654 configurations and valence pion mass used for this calculation.

β	$L^3 \times T$	a (fm)	c_{sw}	κ_l^{sea}	m_π^{sea} (MeV)
3.34	$24^3 \times 48$	0.098	2.066 86	0.136 75	333
			N_{cfg}	κ_l^v	m_π^v (MeV)
			864	0.136 22	547

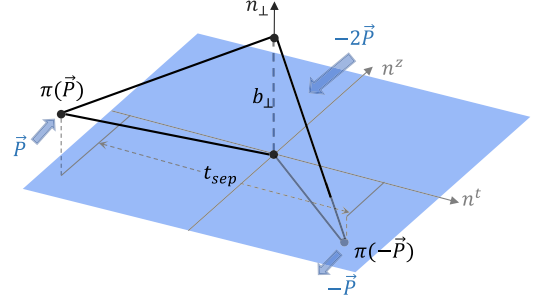


FIG. 1. Illustration of the pseudoscalar meson form factor F calculated in this Letter. The initial and final momenta of the pion are large and opposite. The transition “current” is made of two local operators at a fixed spatial separation b_\perp . t_{sep} is the time separation between the source and sink of the pion.

current made of two quark bilinears with a fixed transverse separation $\vec{b} = (\vec{n}_\perp b_\perp, 0)$,

$$F(b_\perp, P^z) = \langle \pi(-\vec{P}) | (\bar{q}_1 \Gamma q_1)(\vec{b}) (\bar{q}_2 \Gamma q_2)(0) | \pi(\vec{P}) \rangle_c. \quad (2)$$

Here $q_{1,2}$ are light quark fields of different flavors, and $\vec{P} = (\vec{0}_\perp, P^z)$. To extract the soft factor, operators and mesonic states are chosen such that each of the four lines in Fig. 1 are of a different flavor, as pointed out in Ref. [9]. The simplest scenario would correspond to the contraction in Fig. 1, which shares the same topology as the so-called connected insertion; thus, a subscript c is added on the right-hand side of Eq. (2). By construction, the disconnected insertion is not relevant in this scenario that we will adopt in this Letter.

It can be shown that the form factor defined in Eq. (2) is factorizable into the quasi-TMDWF Φ and the intrinsic soft function S_I [9,16]

$$\begin{aligned} F(b_\perp, P^z) &= S_I(b_\perp) \int_0^1 dx dx' H(x, x', P^z) \Phi^\dagger(x', b_\perp, -P^z) \Phi(x, b_\perp, P^z), \end{aligned} \quad (3)$$

where H is the perturbative hard kernel. The quasi-TMDWF Φ is the Fourier transformation of the coordinate-space correlation function

$$\begin{aligned} \phi(z, b_\perp, P^z) &= \lim_{\ell \rightarrow \infty} \frac{\phi_\ell(z, b_\perp, P^z, \ell)}{\sqrt{Z_E(2\ell, b_\perp)}}, \\ \phi_\ell(z, b_\perp, P^z, \ell) &= \langle 0 | \bar{q}_1 \left(\frac{z}{2} n^z + \vec{b} \right) \Gamma_\Phi \mathcal{W}(\vec{b}, \ell) q_2 \left(-\frac{z}{2} n^z \right) | \pi(\vec{P}) \rangle. \end{aligned} \quad (4)$$

In the above, $\mathcal{W}(\vec{b}, \ell)$ is the spacelike staple-shaped gauge link,

$$\begin{aligned} \mathcal{W}(\vec{b}, \ell) &= \mathcal{P} \exp \left[ig_s \int_{-\ell}^{z/2} ds n^z A(n^z s + b_\perp) \right] \\ &\times \mathcal{P} \exp \left[ig_s \int_0^{b_\perp} ds n_\perp A(-\ell n^z + s n_\perp) \right] \\ &\times \mathcal{P} \exp \left[ig_s \int_{-z/2}^{-\ell} ds n^z A(n^z s) \right], \end{aligned} \quad (5)$$

n^z and n_\perp are the unit vectors in z and transverse directions, respectively. $Z_E(2\ell, b_\perp)$ is the vacuum expectation value of a rectangular spacelike Wilson loop with size $2\ell \times b_\perp$, which removes the pinch-pole singularity and Wilson-line self-energy in quasi-TMDWF [9].

Since the UV divergence of the intrinsic soft function is multiplicative [16], the ratio $S_I(b_\perp, 1/a)/S_I(b_{\perp,0}, 1/a)$ calculable on lattice is UV renormalization scheme independent, where $b_{\perp,0}$ is a reference distance that is taken small enough to be calculated perturbatively. Thus, we can obtain the result in the $\overline{\text{MS}}$ scheme through

$$S_{I,\overline{\text{MS}}}(b_\perp, \mu) = \left(\frac{S_I(b_\perp, 1/a)}{S_I(b_{\perp,0}, 1/a)} \right) S_{I,\overline{\text{MS}}}(b_{\perp,0}, \mu), \quad (6)$$

where $S_{I,\overline{\text{MS}}}(b_{\perp,0}, \mu)$ is perturbatively calculable, e.g.,

$$S_{I,\overline{\text{MS}}}(b_\perp, \mu) = 1 - \frac{\alpha_s C_F}{\pi} \ln \frac{\mu^2 b_\perp^2}{4e^{-2\gamma_E}} + \mathcal{O}(\alpha_s). \quad (7)$$

In the present exploratory study, we will consider only leading-order matching in Eq. (3), for which the perturbative kernel is $H(x, x', P^z) = 1/(2N_c) + \mathcal{O}(\alpha_s)$, independent of x and x' . Using $\phi(0, b_\perp, -P^z) = \phi(0, b_\perp, P^z)$ under parity transformation, we obtain

$$S_I(b_\perp) = \frac{2N_c F(b_\perp, P^z)}{|\phi(0, b_\perp, P^z)|^2} + \mathcal{O}(\alpha_s, (1/P^z)^2), \quad (8)$$

where power corrections from finite P^z are ignored. Since P^z is related to the rapidity of the meson, we henceforth replace it by the boost factor $\gamma \equiv E_\pi/m_\pi$. Equation (6) can be written as

$$\begin{aligned} S_{I,\overline{\text{MS}}}(b_\perp, \mu) &= \frac{F(b_\perp, P^z)}{F(b_{\perp,0}, P^z)} \frac{|\phi(0, b_{\perp,0}, P^z)|^2}{|\phi(0, b_\perp, P^z)|^2} \\ &+ \mathcal{O}(\alpha_s, \gamma^{-2}). \end{aligned} \quad (9)$$

The ratio on the right-hand side of the above expression is independent of the renormalization scale μ since only the leading-order contribution is kept.

On the other hand, the quasi-TMDWF can be used to extract the Collins-Soper kernel K using a method similar to [20]

$$K(b_\perp, \mu) = \frac{1}{\ln(P_1^z/P_2^z)} \ln \left| \frac{C(xP_2^z, \mu) \Phi_{\overline{\text{MS}}}(x, b_\perp, P_1^z, \mu)}{C(xP_1^z, \mu) \Phi_{\overline{\text{MS}}}(x, b_\perp, P_2^z, \mu)} \right| \quad (10)$$

$$\begin{aligned} &= \frac{1}{\ln(P_1^z/P_2^z)} \ln \left| \frac{\int_0^1 dx \Phi(x, b_\perp, P_1^z)}{\int_0^1 dx \Phi(x, b_\perp, P_2^z)} \right| + \mathcal{O}(\alpha_s, \gamma^{-2}) \\ &= \frac{1}{\ln(P_1^z/P_2^z)} \ln \left| \frac{\phi(0, b_\perp, P_1^z)}{\phi(0, b_\perp, P_2^z)} \right| + \mathcal{O}(\alpha_s, \gamma^{-2}). \end{aligned} \quad (11)$$

In the second line, again only the leading-order matching kernel $C(xP^z, \mu) = 1 + \mathcal{O}(\alpha_s)$ is used. The renormalization factors for Φ are canceled. The rapidity-scheme-independent CS kernel K is independent of μ in this approximation because only the leading term has been kept.

While Eqs. (6) and (10) are exact and can be used for precision studies in the future, Eqs. (9) and (11) are the leading-order approximation used in this pioneering Letter.

Simulation setup.—For the present study, we use configurations generated with $2 + 1$ flavor clover fermions and tree-level Symanzik gauge action configuration by the CLS Collaboration using periodic boundary conditions [26]. The detailed parameters are listed in Table I. Note that $m_\pi = 547$ MeV instead of 333 MeV is used for valence quarks in order to have a better signal. Physically, the soft function becomes independent of the meson mass for large boost factors γ .

To calculate the form factor in Eq. (2), we generate the wall source propagator,

$$S_w(x, t, t'; \vec{p}) = \sum_{\vec{y}} S(t, \vec{x}; t', \vec{y}) e^{i\vec{p} \cdot (\vec{y} - \vec{x})}, \quad (12)$$

on the Coulomb gauge fixed configurations at $t' = 0$ and t_{sep} for both the initial and final meson states. S is the quark propagator from (t', \vec{y}) to (t, \vec{x}) . Then we can construct the three-point function (3pt) corresponding to the form factor in Eq. (2),

$$\begin{aligned} C_3(b_\perp, P^z; p^z, t_{\text{sep}}, t) &= \frac{1}{L^3} \sum_x \text{Tr} \langle S_w^\dagger(\vec{x} + \vec{b}, t, 0; -\vec{p}) \gamma_5 \Gamma S_w(\vec{x} + \vec{b}, t, t_{\text{sep}}; \vec{p}) \\ &\times S_w^\dagger(\vec{x}, t, t_{\text{sep}}; -\vec{P} + \vec{p}) \gamma_5 \Gamma S_w(\vec{x}, t, 0; \vec{P} - \vec{p}) \rangle. \end{aligned} \quad (13)$$

The quark momentum $\vec{p} = (\vec{0}_\perp, p^z)$ and the relation $\gamma_5 S^\dagger(x, y) \gamma_5 = S(y, x)$ have been applied for the antiquark propagator. We have tested several choices of Γ and will use the unity Dirac matrix $\Gamma = I$ as it has the best signal and describes the leading twist light-cone contribution in the large P^z limit. Notice that the $\Gamma = \gamma_4$ case is subleading in the large P^z limit and is less suitable, although the excited state contamination might be smaller.

By generating the wall source propagators at all the 48 time slices with quark momentum $p^z = (-2, -1, 0, 1, 2) \times 2\pi/(La)$, we can maximize the

statistics of the 3pt function with all the meson momenta P_z from 0 to $8\pi/(La)$ (~ 2.1 GeV) with arbitrary t and t_{sep} . $C_3(b_\perp, P^z, t_{\text{sep}}, t)$ is related to the bare $F(b_\perp, P^z)$ using standard parametrization of 3pt with one excited state,

$$C_3(b_\perp, P^z; p^z, t_{\text{sep}}, t) = \frac{A_w(p_z)^2}{(2E)^2} e^{-Et_{\text{sep}}} [F(b_\perp, P^z) + c_1(e^{-\Delta Et} + e^{-\Delta E(t_{\text{sep}}-t)}) + c_2 e^{-\Delta Et_{\text{sep}}}] \quad (14)$$

A_w is the matrix element of the Coulomb gauge fixed wall source pion interpolation field, $E = \sqrt{m_\pi^2 + P^z{}^2}$ is the pion energy, ΔE is the mass gap between pion and its first excited state, and $c_{1,2}$ are parameters for the excited state contamination. Note that the p_z dependence factor A_w^2 will cancel.

The same wall source propagators can be used to calculate the two-point function related to the bare quasi-TMDWF,

$$C_2(b_\perp, P^z; p_z, \ell, t) = \frac{1}{L^3 \sqrt{Z_E(2\ell, b_\perp)}} \sum_x \text{Tr} e^{i\vec{p}\cdot\vec{x}} \times \langle S_w^\dagger(\vec{x} + \vec{b}, t, 0; -\vec{p}) \mathcal{W}(\vec{b}, \ell) \gamma_5 \Gamma_\Phi S_w(\vec{x}, t, 0; P^z - \vec{p}) \rangle = \frac{A_w(P_z) A_p}{2E} e^{-Et} \phi_\ell(0, b_\perp, P^z, \ell) (1 + c_0 e^{-\Delta Et}), \quad (15)$$

where again we parametrize the mixing with one excited state. A_p is the matrix element of the point sink pion interpolation field. It will be removed when we normalize $\phi_\ell(0, b_\perp, P^z, \ell)$ with $\phi_\ell(0, 0, P^z, 0)$. We choose $\Gamma_\Phi = \gamma^t \gamma_5$ to define the wave function amplitude in Eq. (4). Based on the quasi-TMDPDF study in Refs. [25,27] with a similar staple-shaped gauge link operator, the mixing effect could be sizable when summing various contributions. In the Supplemental Material [28], we report a similar simulation but using the A654 ensemble. We find that the mixing effects can reach order 5% for the transverse separation $b_\perp \sim 0.6$ fm. These effects will be included in the following analysis as one of the systematic uncertainties, while a comprehensive study on the mixing effects will be conducted in the future.

The dispersion relation of the pion state, statistical checks for the measurement histogram, and information on the autocorrelation between configurations can be found in the Supplemental Material [28].

Numerical results.—Figure 2 shows the dependence of the norm of quasi-TMDWFs on the length ℓ of the Wilson line. As one can see from this figure, with $\{P^z, b_\perp, t\} = \{6\pi/L, 3a, 6a\}$, both the quasi-TMDWF $\phi_\ell(0, b_\perp, P^z, \ell)$ and the square root of the Wilson loop Z_E decay exponentially with length ℓ , but the subtracted quasi-TMDWF is length independent when $\ell \geq 0.4$ fm. Some other cases with larger P^z , b_\perp , and t can be found in the Supplemental Material [28]. Based on this observation,

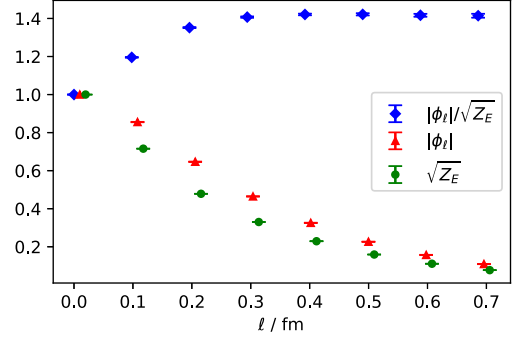


FIG. 2. Results for the ℓ dependence of the quasi-TMDWF with $z = 0$, and also the square root of the Wilson loop which is used for the subtraction, taking the $\{P^z, b_\perp, t\} = \{6\pi/L, 3a, 6a\}$ case as an example. All the results are normalized with their values at $\ell = 0$.

we will use $\ell = 7a = 0.686$ fm as asymptotic results for all cases in the following calculation.

We performed a joint fit of the form factor and quasi-TMDWF with the same P^z and b_\perp with the parametrization in Eqs. (14) and (15). The ratios $C_3(b_\perp, P^z, t_{\text{sep}}, t)/C_2(0, P^z, 0, t_{\text{sep}})$ with different t_{sep} and t for the $\{P^z, b_\perp\} = \{6\pi/L, 3a\}$ case are shown in Fig. 3, with ground state contribution (gray band) and the fitted results at finite t_2 and t (colored bands). In this calculation, the excited state contribution is properly described by the fit with $\chi^2/\text{d.o.f.} = 0.6$. The details of the joint fit, and also more fit quality checks, are shown in the Supplemental Material [28], with similar fitting quality.

The resulting soft factor as a function of b_\perp is plotted in Fig. 4, at $\gamma = 2.17, 3.06$, and 3.98 , which corresponds to $P^z = \{4, 6, 8\}\pi/L = \{1.05, 1.58, 2.11\}$ GeV, respectively. As in Fig. 4, the results at different large γ are consistent with each other, demonstrating that the asymptotic limit is stable within errors. We also compare the intrinsic soft function extracted from the lattice to the one-loop result in Eq. (7), with $\alpha_s(\mu = 1/b_\perp)$ evolving from

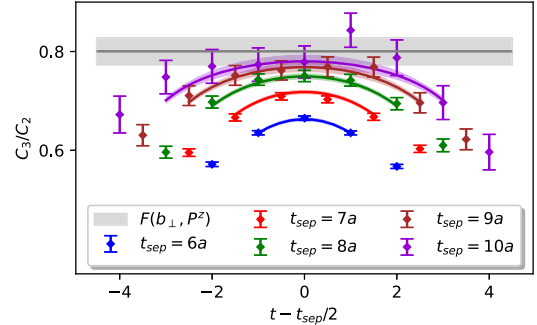


FIG. 3. The ratios $C_3(b_\perp, P^z, t_{\text{sep}}, t)/C_2(0, P^z, 0, t_{\text{sep}})$ (data points) that converge to the ground state contribution at $t, t_{\text{sep}} \rightarrow \infty$ (gray band) as function of t_{sep} and t , with $\{P^z, b_\perp\} = \{6\pi/L, 3a\}$. As in this figure, our data, in general, agree with the predicted fit function (colored bands).

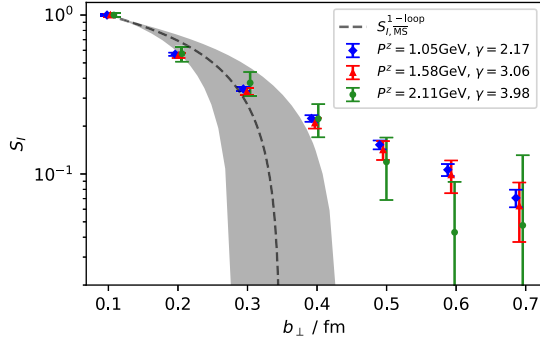


FIG. 4. The intrinsic soft factor as a function of b_{\perp} with $b_{\perp,0} = a$ as in Eq. (9). With different pion momentum P^z , the results are consistent with each other. The dashed curve shows the result of the one-loop calculation [see Eq. (7)], with the strong coupling constant $\alpha_s(1/b_{\perp})$. The shaded band corresponds to the scale uncertainty of α_s : $\mu \in [1/\sqrt{2}, \sqrt{2}] \times 1/b_{\perp}$. The systematic uncertainty from the operator mixing has been taken into account.

$\alpha_s(\mu = 2 \text{ GeV}) \approx 0.3$. The shaded band corresponds to the scale uncertainty of α_s : $\mu \in [1/\sqrt{2}, \sqrt{2}] \times 1/b_{\perp}$. Notice that the b_{\perp} dependence of the former comes purely from the lattice simulation, while that for the latter is from perturbation theory. For ease of comparison, we also tabulate the results for the soft function in the Supplemental Material [28].

We can see a clear P^z dependence in the quasi-TMDWF $|\phi_{\ell}(0, b_{\perp}, P^z, \ell)|$ normalized with $\phi_{\ell}(0, 0, P^z, 0)$, as in the upper panel of Fig. 5. This dependence is related to the CS kernel, as shown in Eq. (11), up to possible LMET matching effects and power corrections of order $1/\gamma^2$. Thus, we use Eq. (11) to extract the kernel in the tree-level approximation and compare the result in the lower panel of Fig. 5 with that of Ref. [25] and up to three-loop perturbative ones with $\alpha_s(\mu = 1/b_{\perp})$. We estimate the systematic uncertainty by combining in quadrature the contributions from the operator mixing effects and from the nonvanishing imaginary part of the quasi-TMDWF, which should be canceled by proper treatments on higher-order effects. For details, see the Supplemental Material [28], in particular Secs. C and F. Our result is consistent with that of Ref. [25].

Summary and outlook.—In this Letter, we have presented an exploratory lattice calculation of the intrinsic soft function by simulating the light-meson form factor of four-quark nonlocal operators and quasi-TMD wave functions. Our result shows a mild hadron momentum dependence, which allows a future precision study to eliminate the large-momentum dependence using perturbative matching [16]. As a reliability check, the agreement between the CS kernel obtained from our quasi-TMDWF result and previous calculations shows that the systematic uncertainties, including the partially quenching effect, the only leading perturbative matching and missing power corrections $1/\gamma$ in LMET expansion, might be subleading. Our calculation

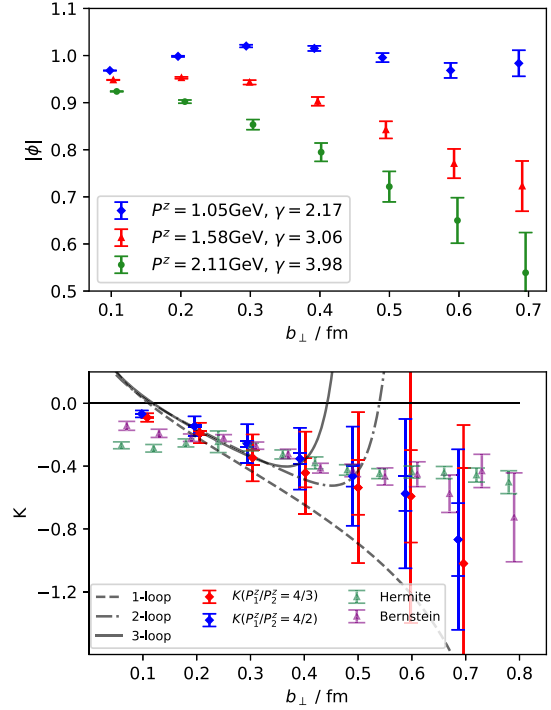


FIG. 5. Quasi-TMDWF (upper) and extracted Collins-Soper kernel (lower), as functions of b_{\perp} . The visible P^z dependence of the quasi-TMDWF can be primarily understood by that from the Collins-Soper kernel, as the kernel we obtained with tree-level matching is consistent with up to three-loop perturbative calculations (at small b_{\perp}) with the strong coupling α_s at the scale $1/b_{\perp}$ and also the nonperturbative result from the pion quasi-TMDPDF. Results based on quenched lattice calculations, labeled as “Hermite” and “Bernstein” [25], are also shown for comparison. Errors in the lower panel correspond to the statistical and systematic errors from the nonzero imaginary part, as well as the operator mixing effects.

paves the way toward the first principle predictions of physical cross sections for, e.g., Drell-Yan and Higgs productions at small transverse momentum.

We thank Xu Feng, Yuan Li, Shi-Cheng Xia, Jianhui Zhang, and Yong Zhao for valuable discussions. We thank the CLS Collaboration for sharing the lattice ensembles used to perform this study. The lattice QCD calculations were performed using the CHROMA software suite [29]. The numerical calculation is supported by Chinese Academy of Science CAS Strategic Priority Research Program of Chinese Academy of Sciences, Grant No. XDC01040100, HPC Cluster of ITP-CAS, and Jiangsu Key Lab for NSLSCS. The setup for numerical simulations was conducted on the π 2.0 cluster supported by the Center for High Performance Computing at Shanghai Jiao Tong University. J.H. is supported by NSFC under Grants No. 11735010 and No. 11947215. Y.-S.L. is supported by National Natural Science Foundation of China under Grant No. 11905126. M. S. and A. S. were supported by the cooperative research

center CRC/TRR-55 of DFG. P.S. is supported by Natural Science Foundation of China under Grant No. 11975127, as well as Jiangsu Specially Appointed Professor Program. W.W. is supported in part by Natural Science Foundation of China under Grants No. 11735010 and No. 11911530088, and by Natural Science Foundation of Shanghai under Grant No. 15DZ2272100. Q.-A.Z. is supported by the China Postdoctoral Science Foundation and the National Postdoctoral Program for Innovative Talents (Grant No. BX20190207).

*Corresponding author.
wei.wang@sjtu.edu.cn

†Corresponding author.
ybyang@itp.ac.cn

- [1] R. K. Ellis, W. J. Stirling, and B. R. Webber, Cambridge Monogr. Part. Phys., Nucl. Phys., Cosmol. **8**, 1 (1996).
- [2] H.-W. Lin *et al.*, *Prog. Part. Nucl. Phys.* **100**, 107 (2018).
- [3] J. C. Collins and D. E. Soper, *Nucl. Phys.* **B193**, 381 (1981); **B213**, 545(E) (1983).
- [4] J. C. Collins, D. E. Soper, and G. F. Sterman, *Nucl. Phys.* **B250**, 199 (1985).
- [5] X.-d. Ji, J.-p. Ma, and F. Yuan, *Phys. Rev. D* **71**, 034005 (2005).
- [6] X.-d. Ji, J.-P. Ma, and F. Yuan, *Phys. Lett. B* **597**, 299 (2004).
- [7] M. G. Echevarria, I. Scimemi, and A. Vladimirov, *Phys. Rev. D* **93**, 054004 (2016).
- [8] Y. Li and H. X. Zhu, *Phys. Rev. Lett.* **118**, 022004 (2017).
- [9] X. Ji, Y. Liu, and Y.-S. Liu, *Nucl. Phys.* **B955**, 115054 (2020).
- [10] X. Ji, *Phys. Rev. Lett.* **110**, 262002 (2013).
- [11] X. Ji, *Sci. Chin. Phys. Mech. Astron.* **57**, 1407 (2014).
- [12] J. Collins, Cambridge Monogr. Part. Phys., Nucl. Phys., Cosmol. **32**, 1 (2011).
- [13] C. W. Bauer, S. Fleming, D. Pirjol, and I. W. Stewart, *Phys. Rev. D* **63**, 114020 (2001).
- [14] C. W. Bauer and I. W. Stewart, *Phys. Lett. B* **516**, 134 (2001).
- [15] C. W. Bauer, D. Pirjol, and I. W. Stewart, *Phys. Rev. D* **65**, 054022 (2002).
- [16] X. Ji, Y.-S. Liu, Y. Liu, J.-H. Zhang, and Y. Zhao, *arXiv:2004.03543*.
- [17] K. Cichy and M. Constantinou, *Adv. High Energy Phys.* **2019**, 3036904 (2019).
- [18] X. Ji, P. Sun, X. Xiong, and F. Yuan, *Phys. Rev. D* **91**, 074009 (2015).
- [19] X. Ji, L.-C. Jin, F. Yuan, J.-H. Zhang, and Y. Zhao, *Phys. Rev. D* **99**, 114006 (2019).
- [20] M. A. Ebert, I. W. Stewart, and Y. Zhao, *Phys. Rev. D* **99**, 034505 (2019).
- [21] M. A. Ebert, I. W. Stewart, and Y. Zhao, *J. High Energy Phys.* **09** (2019) 037.
- [22] X. Ji, Y. Liu, and Y.-S. Liu, *arXiv:1911.03840*.
- [23] A. A. Vladimirov and A. Schäfer, *Phys. Rev. D* **101**, 074517 (2020).
- [24] M. A. Ebert, I. W. Stewart, and Y. Zhao, *J. High Energy Phys.* **03** (2020) 099.
- [25] P. Shanahan, M. Wagman, and Y. Zhao, *Phys. Rev. D* **102**, 014511 (2020).
- [26] M. Bruno *et al.*, *J. High Energy Phys.* **02** (2015) 043.
- [27] P. Shanahan, M. L. Wagman, and Y. Zhao, *Phys. Rev. D* **101**, 074505 (2020).
- [28] See Supplemental Material at <http://link.aps.org/supplemental/10.1103/PhysRevLett.125.192001> for additional informations on data analysis, and also systematic uncertainties from operator mixing and etc.
- [29] R. G. Edwards and B. Joo (SciDAC LHPC, and UKQCD Collaborations), *Nucl. Phys. B, Proc. Suppl.* **140**, 832 (2005).